HEFAT2014
10th International Conference on Heat Transfer, Fluid Mechanics and Thermodynamics
14 – 16 July 2014
Orlando, Florida

COMPUTATIONAL STUDY OF DROPLETS RISING USING LATTICE BOLTZMANN MODEL

Dennis E. Oztekin, Saeed J. Almalowi and Alparslan Oztekin*

*Author for correspondence
Dept. of Mechanical Engineering & Mechanics
Lehigh University
Bethlehem, PA 18015
USA
E-mail: alo2@lehigh.edu

ABSTRACT

Multi relaxation time lattice Boltzmann method is implemented to study unsteady multiphase flows of two immiscible fluids. D2Q9 lattice arrangement for two dimensional flows is employed to investigate lighter fluid droplets rising in heavier fluid. Density distribution functions for each fluid and distribution functions for the coloring step identifying the location of interface separating each immiscible fluid will be used to simulate the dynamics of the droplets and the velocity field of each phase. Buoyancy and other interactive forces between phases are modeled to predict the evolution of droplets as they are rising. No-slip no penetration boundary conditions and periodic boundary conditions are considered in transient flow simulations of multi-phase immiscible fluid for a range of various arrangements of droplets. The effect of the boundaries on the droplets dynamics will be presented.

INTRODUCTION

The present study investigates the nonlinear dynamics of the droplet of the light fluid rising in the heavy fluid. The lattice Boltzmann method is utilized to study multiphase flow. The lattice Boltzmann method has been proven to be an effective method for simulating complex multiphase flow systems [1-3]. Our interest in these flows is to study temporal and spatial characteristics of the lighter fluid droplets as they rise through the heavier fluid. Nonlinear phenomena such as the effect of the boundary have been considered in the present study. The model utilized here to study liquid-liquid multiphase flow includes the interactive forces between fluids.

NOMENCLATURE

f^{σ}	[-]	Distribution function of fluids (σ=1,2)
c	[-]	Lattice discrete velocity
w	[-]	Weight factor
u^{σ}		Total velocity of fluids (σ =1,2) per unit lattice-time step
∅	[-]	Density ratio
κ	[-]	Coloring field
x	[-]	Position vector
t	[s]	Time
x	[m]	Coordinate axis
y	[m]	Coordinate axis
τ^{σ}	[-]	Dimensionless relaxation time for fluids (σ =1,2)
ρ^{σ}	[-]	Macroscopic density of fluids(σ=1,2)
ω^{σ}	[-]	Relaxation frequency of fluids(σ=1,2)
$f^{\sigma eq}$	[-]	Local equilibrium distribution function of fluid (σ=1,2)
δt	[s]	Time step
F_{body}	[N]	Buoyance force
δx	[-]	Distance between two adjacent lattice nodes
Re	[-]	Reynolds number
At	[-]	Atwood number
Eo	[-]	Eotvos number
Mo	[-]	Morton number
G		Dimensionless strength of the interactive forces
μ	[N·s/m^2]	Dynamic Viscosity of fluid
g	[m/s^2]	Gravitational acceleration
υ	[m^2/s]	Kinematic Viscosity

α	[m^2/s]	Thermal diffusivity
α	[-]	Total Number of fluids
∇	[-]	Gradient Operation
δ	[-]	Coloring function

Subscripts

M	[-]	Lattice nodes in x-direction
N	[-]	Lattice nodes in y-direction
k	[W/mK]	Thermal conductivity

GEOMETRY

In this study, different arrangements of droplets have been studied for different boundary conditions, no-slip boundary conditions or periodic boundary conditions. Starting with single droplet is placed on the lower boundary, tow droplets are placed on top of each other's, two droplets are placed side by side, and four droplets are placed in the middle at the same distance form each other's as shown in Figure 1.

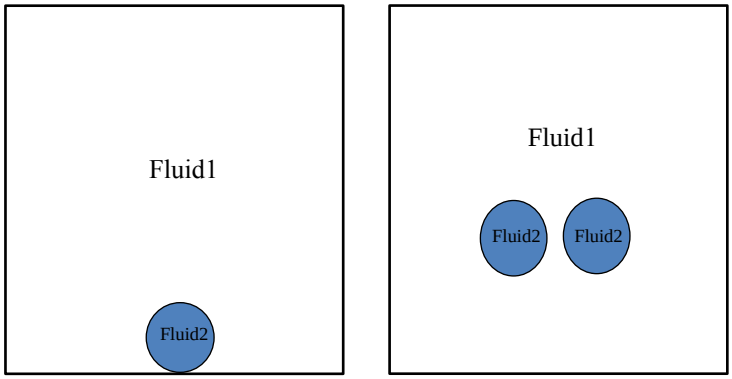

Figure 1. (a) Single droplet sitting at the bottom and **(b)** Two adjacent droplets in the middle. Fluid2 denotes light density while fluid1 denotes heavy density fluid.

NUMERICAL METHOD

The Lattice Boltzmann Method is grounded in kinetic theory. The original theory comes from the Boltzmann equation

$$\frac{\partial f}{\partial t} + \mathbf{c} \cdot \nabla f = \left(\frac{\partial f}{\partial t}\right)_{collision} \quad (1)$$

Equation (1) does not include the external forces. Distribution function, f, is a function of position, r; time, t; and the fluid velocity **c**. f represents the number of particles present at a specific time and position which have a velocity in the neighborhood of v. The complex term at the right side of equation (1) determines the time rate of change of f due to collision. In the 1950s Bhatnagar et al. [4] introduced the approximation:

$$\left(\frac{\partial f}{\partial t}\right)_{colision} = \frac{f^{eq} - f}{\tau} \quad (2)$$

Here f^{eq}, the equilibrium value of fand τ is the lattice relaxation time. For the single relaxation time method τ is described below in terms of lattice viscosity.

$$\tau = 3 * \nu + .5 \quad (3)$$

As it is shown in Succi [5] many of the variables in LBM are understood to be lattice variables. These variables hold the same physical meaning as their real counterparts but have the units of the discretization parameters. The discretization parameters, $\delta_x$and δ_t, are the distance between two consecutive lattices and the time elapsed in one time step, respectively. For example consider the lattice kinematic viscosity shown in equation (3), is given by:

$$\nu = \frac{\delta_t}{\delta_x^2}\frac{1}{R_e} \quad (4)$$

Notice that, just like real kinematic viscosity, the units are time per length squared, because Reynolds number is dimensionless. It can be assumed for the remainder of this paper that all variables with dimensions have been discretized in terms of the lattice discretization parameters. While on the topic of discretization, it seems prudent to discuss the discretization used in the following derivations. In LBM research the lattice studied is typically described by the shorthand DnQm; where n is the number of spatial dimensions and m is the number of lattice direction as each node. Demonstrated in Figure 2 is a typical node in the D2Q9 arrangement, which was used in the present investigation. Once the lattice arrangement is chosen, a number of important parameters can be worked out. The "lattice velocity", $\mathbf{e_k}$, is the expression for the discrete velocity along each lattice branch, k. For the arrangement shown in Figure 2:

$$\mathbf{e_k} = c\{(0,0),(1,0),(-1,0),(0\text{-}1),(1,1),(-1,1),(-1,-1),(1,-1) \quad (5)$$

where **c** is the lattice speed, which is simply δ_x/δ_t. The weighting function is also determined once the arrangement is selected. For this arrangement
$w_k = 1/36\{16, 4, 4, 4, 4, 1, 1, 1, 1\}$.

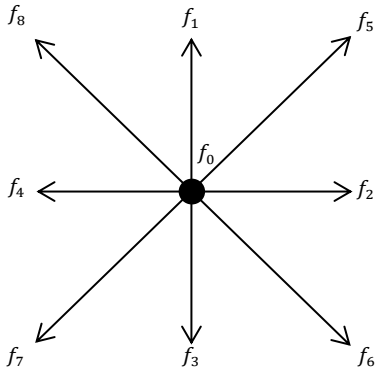

Figure 2. D2Q9 lattice arrangement

From equations 1 and 2, the single relaxation time governing equation, the evolution equation, can be shown to be:

$$f_k(\mathbf{x} + \mathbf{e_k}\delta_t, t + \delta_t) - f_k(\mathbf{x}, t) = -\frac{1}{\tau}\left[f_k(\mathbf{x}, t) - f_k^{eq}(\mathbf{x}, t)\right] \quad (6)$$

This is, of course, an explicit method. At each time step f_k is determined from the previous value of f_k and the updated value of f_k^{eq}. The equilibrium value of f is an important parameter because it is used to force the conservation laws. The Chapman-Enskog expansion developed in Chapman and Cowling [6], is used as the base for the equilibrium distribution function. Here it is with the first three terms, which is all that is needed here:

$$f_k^{eq} = C\left\{1 + C_1\mathbf{e_k}\cdot u + C_2\left[(\mathbf{e_k}\cdot\mathbf{u})^2 - \frac{1}{2}|\mathbf{u}|^2\right] + \cdots\right\} \quad (7)$$

where $\mathbf{u}$ is the fluid velocity. Now these three general constants (C, C_1,C_2) are used to force the three constraints from kinetic theory:

$$\sum_k f_k^{[0]} = \rho \quad \text{and} \quad \sum_k f_k^{[0]}\mathbf{e_k} = \rho u \quad (8)$$

It has been shown in He and Lou [7] that these constraints will force the evolution equation to satisfy the Navier-Stokes equation. Solving for the three general constants using these constraints gives;

$$f_k^{eq} = \rho w_k\left\{1 + \left(3\frac{\mathbf{e_k}\cdot\mathbf{u}}{c^2} + \frac{9}{2}\frac{(\mathbf{e_k}\cdot\mathbf{u})^2}{c^4} - \frac{3}{2}\frac{|\mathbf{u}|^2}{c^2}\right)\right\} \quad (9)$$

where w_k is the weight factor. LBM has shown itself to be very adept at modelling multiphase flows as shown by Hou et al [8]. It completely avoids the hassle of interface tracking which slows down classical methods. To deal with multiple fluids simply introduce multiple density distribution functions: f_k^{σ}, with $\sigma = \{1 \ldots j\}$ where j is the number of fluids in the system. Now the evolution equation becomes the system of equations:

$$f_k^{\sigma}(\mathbf{x} + \mathbf{e_k}\delta_t, t + \delta_t) - f_k^{\sigma}(\mathbf{x}, t) = -\frac{1}{\tau^{\sigma}}\left[f_k^{\sigma}(\mathbf{x}, t) - f_k^{\sigma eq}(\mathbf{x}, t)\right] \quad (10)$$

As it is, this evolution equation is missing a key component to multiphase flows, inter-particle forces, $\mathbf{F}_{int}$. To add this effect into our model we used the model introduced by Shan and Chen [9]. As was mentioned earlier:

$$\sum_k f_k^{\sigma[0]} = \rho^{\sigma} \quad \text{and} \quad \sum_k f_k^{\sigma[0]}\mathbf{e_k} = \rho^{\sigma}\mathbf{u}^{\sigma} \quad (11)$$

Now we also need a common velocity which can be found by what is effectively mass averaging:

$$\mathbf{u}^{\sigma} = \frac{\sum_{\sigma=1}^{j}\frac{\rho^{\sigma}\mathbf{u}^{\sigma}}{\tau^{\sigma}}}{\sum_{\sigma=1}^{j}\frac{\rho^{\sigma}}{\tau^{\sigma}}} \quad (12)$$

With this we can solve for an equilibrium velocity. Using this velocity in the calculations for $f_k^{\sigma eq}$ will automatically account for the inter-particle forces as demonstrated in Shan and Chen [9].

$$\rho^{\sigma}\mathbf{u}^{\sigma eq} = \rho^{\sigma}\mathbf{u}^{\sigma} + \tau^{\sigma}\mathbf{F}^{\sigma} \quad (13)$$

Here $\mathbf{F}^{\sigma}$ is the total inter-particle force on fluid σ per unit volume, but it has been shown by Huang et al [10] that $\mathbf{F}^{\sigma}$ can be extended to include other forces such as body forces and adhesion forces. In the present investigation adhesion forces were ignored; however, a body force, gravity, was included. This was necessary since, modelling of a rise of a lighter fluid droplet in a heavier fluid requires a body force in the opposite direction to a density gradient. Therefore, in the present investigation

$$\mathbf{F}^{\sigma} = \mathbf{F}_{int}^{\sigma} + \mathbf{F}_{body}^{\sigma} \quad (14)$$

The inter-particle force is calculated using an interaction potential function:

$$V(x, x') = G^{\sigma\bar{\sigma}}(\mathbf{x}, \mathbf{x}')\psi^{\sigma}(\mathbf{x})\psi^{\bar{\sigma}}(\mathbf{x}')$$

Where $\mathbf{x}$ and $\mathbf{x}'$ are the position vectors of any two points in the flow domain and $\psi^{\sigma}$is the mass density function. The function $G^{\sigma\bar{\sigma}}(\mathbf{x}, \mathbf{x}')$ is a Green's function. Here only interactions between a point in the fluid and the adjacent point are considered so $G^{\sigma\bar{\sigma}}(\mathbf{x}, \mathbf{x}')$ reduces too:

$$G^{\sigma\bar{\sigma}}(\mathbf{x}, \mathbf{x}') = \begin{cases} 0, & |\mathbf{x} - \mathbf{x}'| > c \\ G, & |\mathbf{x} - \mathbf{x}'| \le c \end{cases}$$

where G is a constant parameter which controls the strength of the inter-particle forces. Now that the effecting area is in the immediate neighborhood, the general position variable, $\mathbf{x}'$, is reduced to $\mathbf{x}^k$ which is the position vector for the nodes next to $\mathbf{x}$ in the direction of k. With the interaction potential known and $G^{\sigma\bar{\sigma}}(\mathbf{x}, \mathbf{x}')$ defined in such a simple way, the interactive force becomes:

$$\mathbf{F}_{int}^{\sigma}(\mathbf{x}) = -\psi^{\sigma}(\mathbf{x})\sum_{\bar{\sigma}=1}^{j} G^{\sigma\bar{\sigma}}(\mathbf{x}, \mathbf{x}^{\mathbf{k}})\sum_{k=1}^{m}\psi^{\bar{\sigma}}(\mathbf{x}^{\mathbf{k}})(\mathbf{x}^{\mathbf{k}} - \mathbf{x}) \quad (15)$$

Now all that remains is to calculate the effective mass which is:

$$\psi^{\sigma} = \rho_0^{\sigma}\left(1 - e^{-\rho^{\sigma}/\rho_0^{\sigma}}\right) \quad (16)$$

$\rho_0^{\sigma}$is the constant density of fluid σ. The gravity force is much simpler:

$$\mathbf{F}_{body}^{\sigma} = \mathbf{g}\rho^{\sigma} \quad (17)$$

For the sake of presentation a coloring step can be added to this method in the two fluid cases. The idea is to create a function k which is one at a node entirely dominated by the lighter fluid, negative one at a node entirely dominated by the heavier fluid, and somewhere between one and negative one for a node which consists of both the light and heavy fluid.

$$\kappa = \frac{\rho^{light} - \rho^{heavy}}{\rho^{light} + \rho^{heavy}} \quad (18)$$

At any given instant this coloring function can be contour plotted to produce an image showing where each fluid is.

The standard single relaxation time LBM discussed above is known to have stability issues at high speed flows that can be seen in multiphase flow studied here with large density differences. To deal with these issues Multi Relaxation Time Lattice Boltzmann Method (MRTLBM) was developed. Consider the vector equation:

$$\mathbf{f}(\mathbf{x} + \mathbf{e}_k\delta_t, t + \delta_t) - \mathbf{f}(\mathbf{x}, t) = S[\mathbf{f}(\mathbf{x}, t) - \mathbf{f}^{eq}(\mathbf{x}, t)] \quad (19)$$

Here f_k and f_k^{eq} have been rewritten as f and f^{eq}which are

vectors of dimension k. Notice that when the collision matrix is defined as

$$S = \frac{1}{\tau} I \tag{20}$$

where **I** is the identity matrix, the equation reduces to the single relaxation time LBM evolution equation. The idea in MRTLBM is to convert the right hand side of this equation from velocity space to moment space using the linear mapping:

$$m = M \cdot f \tag{21}$$

Then defining, $\hat{S} = M \cdot S \cdot M^{-1}$ the evolution equation becomes:

$$f_k(\mathbf{x} + \mathbf{e_k}\delta_t, t + \delta_t) - f_k(\mathbf{x}, t) = -M^{-1}\hat{S}\left[m_k(\mathbf{x}, t) - m_k^{eq}(\mathbf{x}, t)\right] \tag{22}$$

For a more detailed derivation see the work of d'Humieres and his colleagues [11, 12].

In the present study the moment transformation matrix and the equilibrium moment are selected as

$$M = \begin{bmatrix} 1 & 1 & 1 & 1 & 1 & 1 & 1 & 1 & 1 \\ -4 & -1 & -1 & -1 & -1 & 2 & 2 & 2 & 2 \\ 4 & -2 & -2 & -2 & -2 & 1 & 1 & 1 & 1 \\ 0 & 1 & 0 & -1 & 0 & 1 & -1 & -1 & 1 \\ 0 & -2 & 0 & 2 & 0 & 1 & -1 & -1 & 1 \\ 0 & 0 & 1 & 0 & -1 & 1 & -1 & -1 & 1 \\ 0 & 0 & -2 & 0 & 2 & 1 & 1 & -1 & -1 \\ 0 & 1 & -1 & 1 & -1 & 0 & 0 & 0 & 0 \\ 0 & 0 & 0 & 0 & 0 & 1 & -1 & 1 & -1 \end{bmatrix}$$

$$m^{eq} = \begin{bmatrix} \rho \\ -2\rho + 3\left(J_x^2 + J_y^2\right) \\ \rho - 3\left(J_x^2 - J_y^2\right) \\ J_x \\ -J_x \\ J_y \\ -J_y \\ \left(J_x^2 - J_y^2\right) \\ J_x J_y \end{bmatrix} \tag{23}$$

where Jx and Jy are linear momentum in x and y directions. Components of the diagonal matrix $\hat{S}$ are 1, 1.4, 1.4, 1, 1.2, 1, 1.2, 1/ω and 1/ω.

In the present investigation a mass conserving boundary contention treatment similar to the one studied by Zou and He [13] and Kuo and Chen [14] is employed. The idea in this method is to derive the three directions facing away from the boundary from the set of equations formed by: the conservation of mass, the conservation of momentum (equation (8)), and the non-equilibrium bounce back condition. The non-equilibrium bounce back condition states that the part of the density distribution function not contributing to the equilibrium will be reflected from the boundary. Therefore:

$$f_a - f_a^{eq} = f_b - f_b^{eq} \tag{24}$$

where the direction b is opposite of a. In the no slip no penetration case shown in Figure 3 this generates:

$$\begin{aligned} f_1 &= f_3 \\ f_5 &= f_7 - \frac{1}{2}(f_2 - f_4) \\ f_8 &= f_6 + \frac{1}{2}(f_2 - f_4) \end{aligned} \tag{25}$$

In this study all boundaries are no slip and no penetration type, so treatment for each boundary looks similar to this with the direction changed.

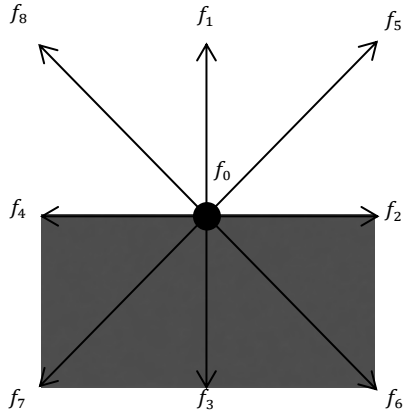

Figure 3. D2Q9 arrangement for the lattice located on the bottom boundary

RESULTS AND DISCUSSIONS

In images shown below, red color denotes the higher density fluid while blue color denotes the lower density fluid. A 300×300 node lattice is sufficient to provide spectral convergence in all simulations presented here. Since the lattice spacing and the time steps are related in the lattice Boltzmann method through the lattice speed, c; the corresponding time step of 0.00015 sec is sufficient to provide temporal convergence.

Both no-slip and periodic types of boundary conditions are imposed at lower and upper boundaries. For the time steps and the spacing between the lattices selected in the present simulations, the relaxation frequency, inverse of relaxation time, for lighter fluid (water is selected as a lighter fluid) is ω_1=0.5657 and for the heavier fluid (oil is selected as a heavier fluid) is ω_2=1.3815. The strength of the inter-particle forces is selected to be -1.2. The density ratio of fluids is 1.2 and the Atwood number, A=$\frac{\rho_h - \rho_l}{\rho_h + \rho_l}$ ~0.1 where ρ_h and ρ_l are densities of the heavier and the lighter fluids, respectively. The Atwood number of this flow corresponds to the Reynolds number $Re = \frac{vd}{\upsilon}$, where d is the initial diameter of the droplet (selected as 0.04 m), υ is the kinematic viscosity of the heavier fluid and v is the terminal speed of the droplet.

Figure 4 shows density contours at various times for a single droplet placed at the bottom of the boundary at t = 0. The no-slip boundary condition is imposed on the velocity field at the

bottom boundary. It is noted that the droplet is attached to the boundary at a single point. At time t = 0.071 sec the droplet is slightly elongated in the direction of gravity and it is still in contact with the boundary. At a later time the droplet rises above the boundary and at the tail of the droplet streaks of the lighter fluid extend to the surface. The back side of the droplet is nearly flat with a small dimple at the center region of the back side. At t = 1.57 sec the tail is completely broken and the droplet assumes the shape of the crescent, caused by the faster rise of the bottom compared to the front and side section of the droplet. The effect of the boundary on the dynamics of the droplet is obvious but not that strong. This is due to the fact that the droplet touches to the boundary at a single point. More pronounced effects of the no-slip boundary would have been realized if a larger portion of the droplet was in contact with the boundary.

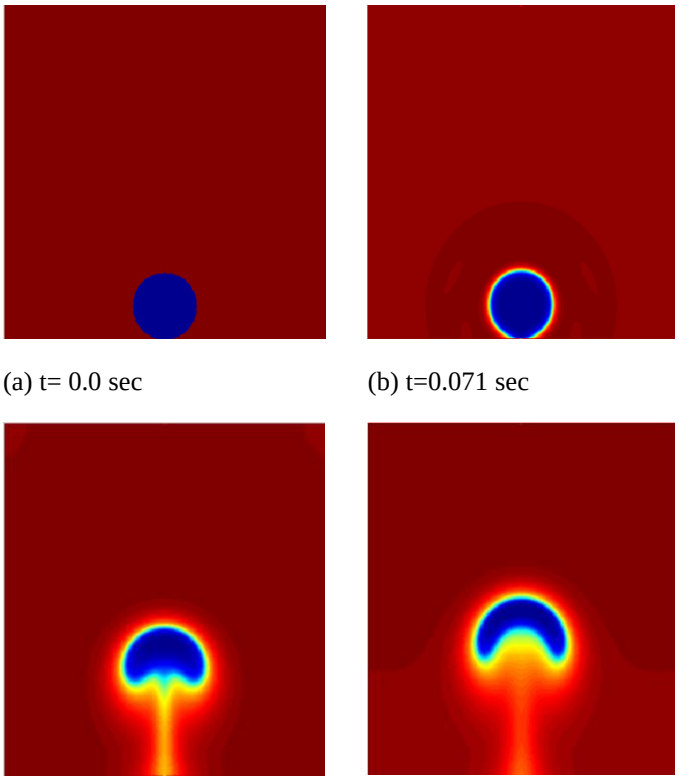

(a) t= 0.0 sec (b) t=0.071 sec

(c) t=1.35 sec (d) t=1.57 sec

Figure4. Density contour of a single rising droplet with a no-slip condition at the bottom boundary at various times.

Figure 5 shows the density contours of a rising lighter fluid droplet in a heavier fluid with periodic top and bottom boundary conditions. The crescent shaped droplet at the later stages of the flow is seen due to non-uniform rising rate of the droplet. The back side of the droplet rises faster compared to the front side leading the shape predicted at later stage, as seen in both Figures 4 and 5. The topology of the back side of the droplet is simpler and more uniform and the extended tail is not present at any stage of the flow.

The Morton, Eötvös and Reynolds numbers determine the spatial structure of the droplet as it approaches to its terminal speed [15,16]. In order to illustrate this, the droplet speed at t = 1.35 s is used to calculate these dimensionless groups. For the droplet speed 0.0296 m/sec at t = 1.35 sec Re=1184, $Eo = \frac{\rho d^2 g}{G_s} = 58$ and $Mo = \frac{g v^4 \rho^4}{{G_s}^3} = 3.38 \times 10^{-11}$. Here G_s is the scale of the surface tension. It is documented by Benzi et al. [17] that Gs ≈ −1/(3G). The crescent shape for the droplet is expected at these flow regimes, as shown in the Figure 4c. The shear stress along the surface of the droplet varies depending on the local velocity of the water passing across the oil surface. Because the interactive forces are constant in magnitude, the variances in shear forces create a slight instability in the droplet, which in turn causes the droplet takes the shape of a crescent.

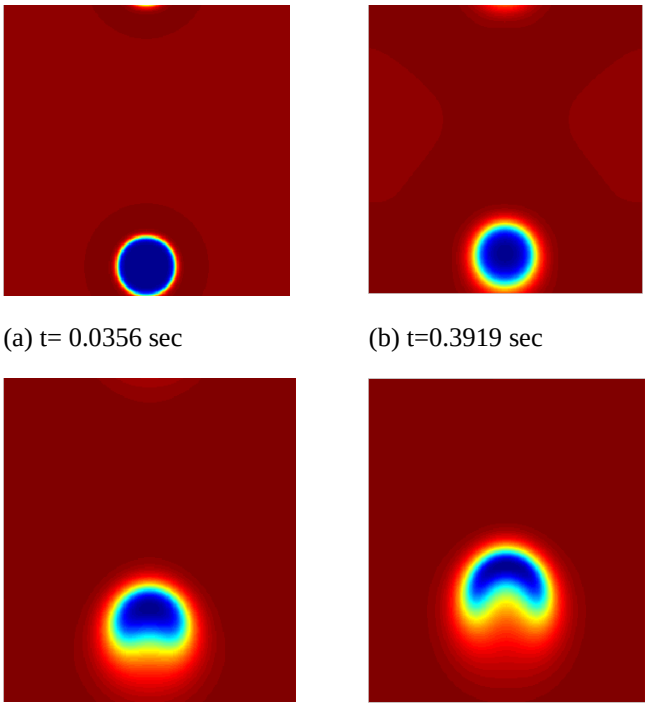

(a) t= 0.0356 sec (b) t=0.3919 sec

(c) t=0.463 sec (d) t=0.677 sec

Figure5. Density contour of a single rising droplet with a periodic top and bottom boundary conditions at various times

Figure 6 shows the density contours of the two droplets placed side by side at t = 0. Periodic boundary conditions are adopted at the upper and lower boundaries. The droplets are circular in shape originally. Soon after the droplets are released they are slightly distorted; becoming a slightly tilted ellipse, as shown in Figure 6b. At later stages the crescent shape of droplets has

distorted significantly making pointy bottom edge at the sides facing each other.

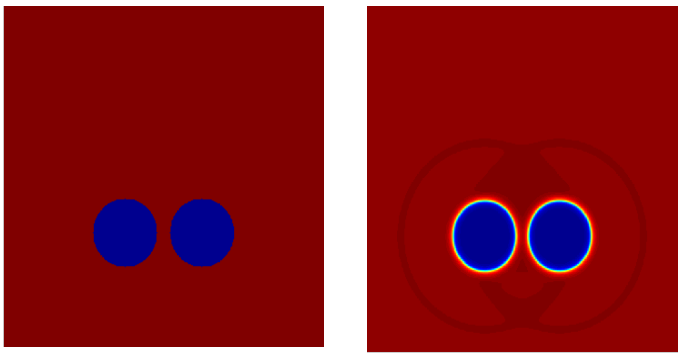

(a) t= 0.0 sec (b) t=0.0384 sec

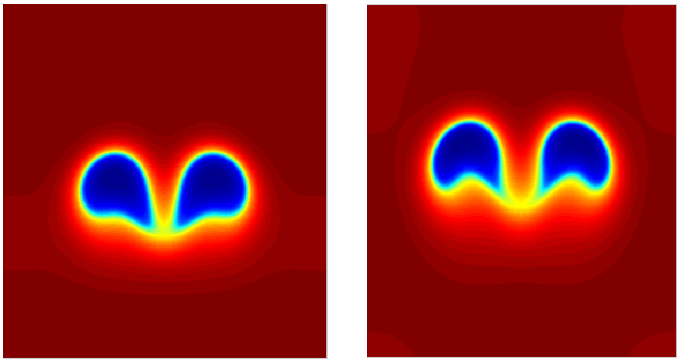

(c) t=0.285 sec (d) t=0.677 sec

Figure 6. Density contour of two rising droplets originally placed side by side with a periodic top and bottom boundary conditions at various times

CONCLUSION

D2Q9 MRT-Lattice Boltzmann method is implemented to study a light droplet rising in a heavier fluid. Density distribution functions for each fluid and the function for the coloring step to identify the location of interface separating each immiscible fluid is determined at various stages. The effect of the BCs is investigated as well. The evolution of the interface is captured naturally by the Lattice Boltzmann method. This study proves that Lattice Boltzmann method could be an effective computational fluid dynamics (CFD) tool to simulate multi-phase flows and interfacial phenomena.

ACKNOWLEDGEMENT

The authors would like to acknowledge the support of Saudi government and Taibah University for the scholarship provided for SJA.

REFERENCES

[1] M. Cheng, J. Hua, and J Lou, 2010, Simulation of Bubble-Bubble Interaction Using a Lattice Boltzmann Method., *Computers & Fluid*, 39, 260-270

[2] S. Chen and G. D. Doolen, 1998, Lattice Boltzmann Method for Fluid Flows., *Annu. Rev. Fluid Mech*,30,329-364

[3] S. J. Almalowi, D. E. Oztekin, and A. Oztekin, 2013, Rayleigh-Taylor Instability Studied with Multi-relaxation Lattice Boltzmann Method., *ASME Conference Proceeding IMECE*

[4] P.L. Bhatnagar, E.P. Gross, and M. Krook, 1954, A Model for Collision Processes in Gases. I. Small Amplitude Processes in Charged and Neutral One-Component Systems., *Physical Review*, 94(3), 511-525

[5] S. Succi, 2001, The Lattice Boltzmann Equation for Fluid Dynamics and Beyond., Oxford Science Publications

[6] S. Chapman, and T. G. Cowling, 1999, The Mathematical Theory of Non-Uniform Gases., Digital Edition, Cambridge Mathematical Library

[7] X. He, and L. Luo, 1997, Lattice Boltzmann Model for the Incompressible Navier-Stokes Equation., *Journal of Statistical Physics*, 88(3)

[8] S. Hou, X. Shan, Q. Zou, G. Doolen, and W.E. Soll, 1997, Evaluation of Two Lattice Boltzmann Models for Multiphase Flows., *Journal of Computational Physics*, 138, 695-713

[9] X. Shan, and H. Chen, 1993, Lattice Boltzmann Model for Simulating Flows with Multiple Phases and Components., *Physical Review E*., 47(3), 1815-1819

[10] H. Huang, Z. Li, S. Lui, and Z. Lu, 2009, Shan-and-Chen-type Multiphase Lattice Boltzmann Study of Viscous Coupling Effects for Two-Phase Flow in Porous Media., *International Journal for Numerical Methods in Fluids*, 61, 341-354

[11] D. d'Humieres, I. Ginzburg, M. Krafczyk, P. Lallemand, and L. Luo, 2002, Multiple-Relaxation-Time Lattice Boltzmann Models in Three Dimensions., *Philosophical Transactions Royal Society of London A*,360, 437-451

[12] D. d'Humieres, 1992, Generalized Lattice Boltzmann Equations., Rarefied Gas Dynamics Theory and Simulations, 159,450-458

[13] Q. Zou, and X. He, 1997, On Pressure and Velocity Boundary Conditions for the Lattice Boltzmann BGK Model., *Physics of Fluids*, 9, 1591

[14] L. S. Kuo, and P. H. Chen, 2008, A Unified Approach for Nonslip and Slip Boundary Conditions in the Lattice Boltzmann Method., *Computers & Fluids*, 38, 883-887

[15] D. Bhaga and M.E. Weber, 1981, Bubbles in Viscous Fluids: Shape, Wakes and Velocities, Journal of Fluid Mechanics, 105, 61-85

[16] L. Chen, S.V. garimella, J.A Reizes and E. Leonard, 1999, The Development of a Bubble Rising in a Viscous Fluid, Journal of Fluid Mechanics, 387, 61-96

[17] R. Benzi, L. Biferale, M Sbragaglia, S. Succi, and F. Toschi, 2006, Mesoscopic Modeling of a Two-phase in the Presence of Boundaries: The Contact Angle, Phys. Rev. E, 021509